Available online at www.sciencedirect.com
SCIENCE DIRECT®
Journal of Hydrology 285 (2004) 177–198
Journal of Hydrology
www.elsevier.com/locate/jhydrol

# Hydrologic and geologic factors controlling surface and groundwater chemistry in Indian Wells-Owens Valley area, southeastern California, USA

Cüneyt Güler[a], Geoffrey D. Thyne[b,*]

[a]*Mersin Üniversitesi, Çiftlikköy Kampüsü, Jeoloji Mühendisliği Bölümü, 33343 Mersin, Turkey*
[b]*Colorado School of Mines, Department of Geology and Geological Engineering, 1500 Illinois Street, Golden, CO 80401, USA*

Received 28 February 2002; accepted 19 August 2003

**Abstract**

The Indian Wells-Owens Valley area is located in the semi-arid Basin and Range province, which is characterized by alternating mountains and alluvial basins. Surface water resources are limited in this arid region and water demand is mainly met by groundwater pumpage. In a classic Basin and Range groundwater system, water flows from recharge areas in the mountains to discharge areas in adjacent valleys. Discharge areas are generally occupied by playas where large amounts of salt deposition occur due to evaporating groundwater.

Hydrochemical data from a total of 1368 spring, surface, and well water samples collected over an 80-year period were used to evaluate water quality and to determine processes that control water chemistry. Q-mode hierarchical cluster analysis (HCA) was employed for partitioning the water samples into hydrochemical facies, also known as water groups or water types. Five major water groups resulted from the HCA analysis. The samples from the area were classified as recharge area waters ($Ca-Na-HCO_3$ water and $Na-Ca-HCO_3$ water), transition zone waters ($Na-HCO_3-Cl$ water), and discharge area waters (Na–Cl water and more concentrated Na–Cl water). Spatial plots of the major statistical groups show that the samples that belong to the same group are located in close proximity to one another suggesting the same processes and/or flowpaths. Inverse geochemical models of the statistical groups were developed using PHREEQC to elucidate the chemical reactions controlling water chemistry. The inverse geochemical modeling demonstrated that relatively few phases are required to derive water chemistry in the area. In a broad sense, the reactions responsible for the hydrochemical evolution in the area fall into four categories: (1) silicate weathering reactions; (2) dissolution of salts; (3) precipitation of calcite, amorphous silica, and clay minerals; and (4) ion exchange.


*Keywords:* Water chemistry; Cluster analysis; Geochemical modeling; PHREEQC; Basin and range; California

## 1. Introduction

The Indian Wells-Owens Valley area is located in a relatively unpopulated region, which is currently undergoing a significant increase in water demand.

* Corresponding author. Tel.: +1-303-273-3104; fax: +1-303-273-3859.
*E-mail address:* gthyne@mines.edu (G.D. Thyne).

0022-1694/$ - see front matter © 2003 Elsevier B.V. All rights reserved.
doi:10.1016/j.jhydrol.2003.08.019

In the study area, there are a wide variety of climatic conditions, hydrologic regimes, and geologic environments. Thus, the water samples from the area represent a variety of water types having a wide range of chemical composition. Due to both the complexity of the groundwater flow system and the overall lack of hydrochemical and hydrologic data for much of the region, large uncertainties exist in the current groundwater flow models. The complex system is complicated by heavy pumping from valley aquifers for agricultural and public use, disposal of treated wastewater and possible groundwater flow barriers.

Previous studies have shown that major-ion chemistry of natural waters can often be explained by the reaction of these waters with rocks or sediments through which they flow (Back, 1966; Garrels and MacKenzie, 1967; White et al., 1980; Frape et al., 1984; Hem, 1989; Thomas et al., 1989). The spatial variability observed in the composition of these natural tracers can provide insight into aquifer heterogeneity and connectivity as well as the physical and chemical processes controlling water chemistry. As a result, the use of major-ions as natural tracers has become an accepted method to delineate flowpaths in aquifers. Generally, the approach is to divide the samples into hydrochemical facies, that is group samples with similar chemical characteristics that can then be correlated with location. Verification that systematic variations along the flowpath are related to reactions between groundwater and the aquifer provides the hydrochemical evolution model for the area. This information provides the context for interpreting the spatial variations in water chemistry and defining groundwater flowpaths.

In this study, physical, hydrogeologic, and hydrochemical information from the groundwater system will be integrated and used to determine the main factors and mechanisms controlling the chemistry of surface and groundwaters in the area. The main issues that will be addressed by this study include: (1) the validity of statistical clustering techniques in classifying the samples into hydrochemical facies on a regional scale; (2) development of a hydrochemical model for the region; (3) the relative importance of hydrologic and geologic factors in controlling the water chemistry; and (4) the assessment of the value of this approach to delineate flowpaths.

## 2. Description of the study area

The study area lies within the south Lahontan hydrologic region, California, and covers approximately 29,800 km$^2$ stretching from Owens Valley (OV) in the north to Indian Wells Valley (IWV) in the south (Figs. 1 and 2). These valleys are young, complex structural and topographic depressions and are tectonically similar to other valleys in the Basin and Range physiographic province. Both OV and IWV are bordered on the west by the Sierra Nevada with peaks rising from 1829 to 4417 m and on the east by several ranges including the Inyo Mountains, the Coso Range, and the Argus Range with elevations ranging from 1500 to 2750 m. Topography of the valley floors is relatively flat and slopes to the south with elevations decreasing from 1100 m in the OV to nearly 663 m in the vicinity of IWV.

The existing topographic relief between the ranges (horsts) and the valley floors (grabens) of the area is mostly the result of the tectonic activity and faulting that occurred during the Late Cenozoic time (Christensen, 1966). The area lies in close proximity to several major active fault zones of California

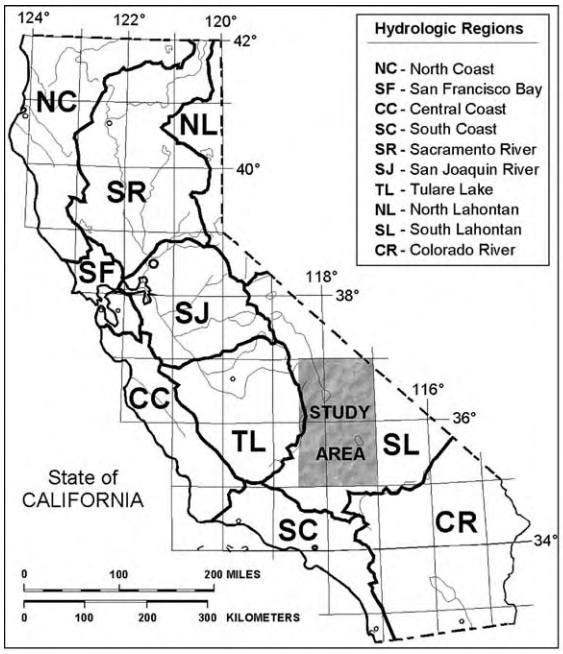


Fig. 1. Location of the study area showing the hydrologic regions of California.

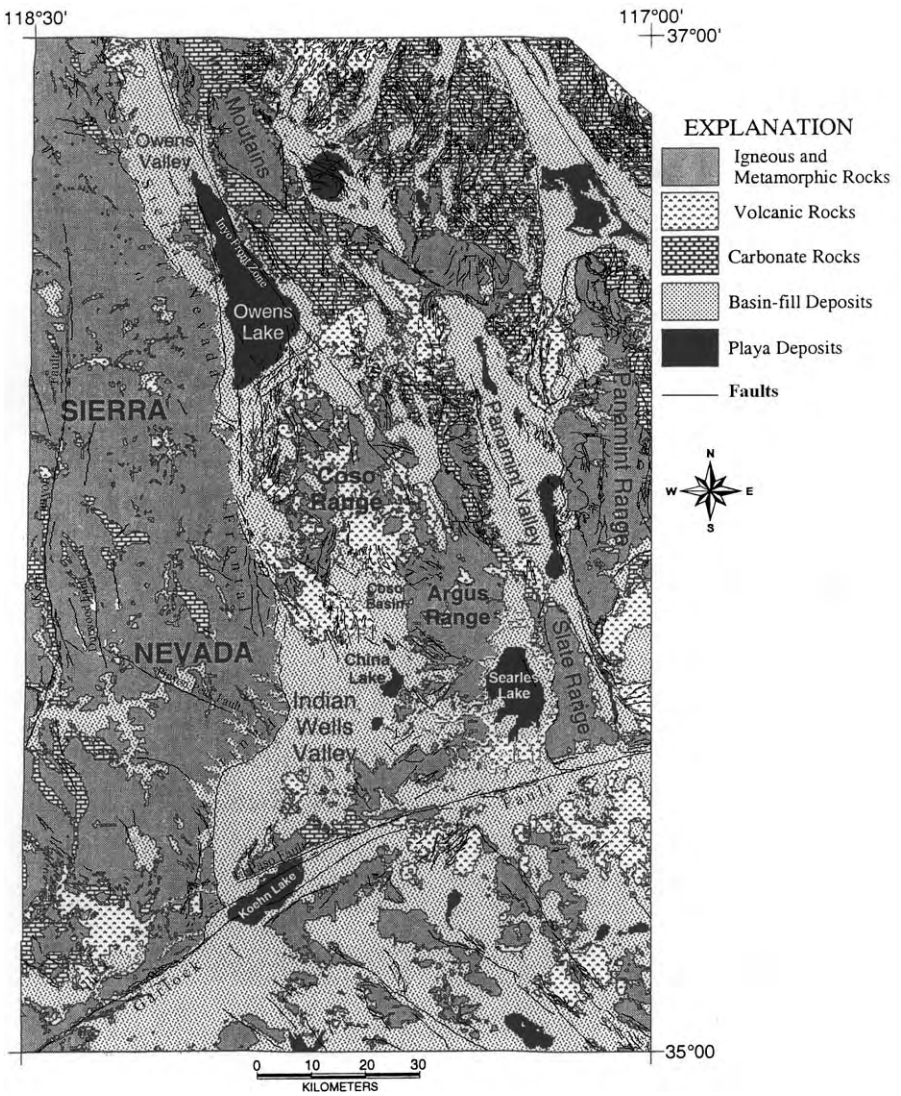


Fig. 2. Map of rock types and general features of the Indian Wells-Owens Valley area, California.

including the San Andreas fault (150 km to the southwest), the Sierra Nevada frontal fault, Kern Canyon fault, Death Valley-Furnace Creek fault zone, Garlock fault, and Argus fault. Locally, complex faulting occurs in all the bordering ranges (Fig. 2). Several major, and numerous minor local faults that propagate upwards from the underlying crystalline basement dissect the basin-fill deposits. The majority of these structural discontinuities have been determined by the aid of seismic refraction and gravimetric studies (e.g. von Huene, 1960; Zbur, 1963).

Two contrasting climate regimes exist in the area. High alpine to alpine climate conditions prevail in the Sierra Nevada, which serves as the main recharge area, and arid climate conditions dominate in the adjoining alluvial-filled basins. Climate of the area is mostly shaped by the Sierra Nevada range, which forms a barrier to passing storms and creates a rain shadow effect (Feth et al., 1964a; Whelan et al., 1989). As a result, the mountain ranges in the area generally receive progressively less precipitation from west to east. Average rainfall on the valley floors ranges from

about 75–152 mm, whereas at the crest of the Sierra Nevada average annual precipitation generally varies from 508 to 1400 mm and occurs mostly as snowfall (accounting for 90–95% of the regional precipitation). The large altitude variations affect the temperatures considerably. Average air temperature in the valleys range from 3 °C in winter to 28 °C in summer. Strong winds (annually averaging 13.2 km $h^{-1}$ in China Lake) occur in the late winter and spring as a result of rapidly moving cold frontal systems (Corbett, 1990). These winds occasionally cause severe dust and sandstorms that can significantly reduce visibility (Corbett, 1990) and pose health risks to humans (Saint-Amand, 1986).

### 2.1. Lithology and mineralogy

The chemical composition of minerals in the mountain ranges and basin-fill imposes a fundamental constraint on the selection of the mineral phases that will be used in geochemical calculations. Rocks and unconsolidated deposits in the area can be divided into five hydrogeologic units: (1) igneous and metamorphic rocks; (2) volcanic rocks; (3) carbonate rocks; (4) basin-fill deposits; and (5) playa deposits (Fig. 2). Chemical analyses of the rock types from various parts of the region are presented in Table 1.

Igneous rocks of Mesozoic age outcrop in many mountain ranges and underlie most of the region at depth (Kistler et al., 1965; McKee and Nash, 1967). The granitic rocks range from gabbro to quartz monzonite in composition, with quartz diorite making up the bulk of the plutonic rock (Oliver, 1977). These rocks are characterized by porphyritic texture, phenocrysts of quartz, biotite, plagioclase, K-feldspar (orthoclase), hornblende, olivine, and commonly contain mafic inclusions. Metamorphic rocks of Precambrian age are scattered throughout the area and display very limited areal extension. Together, igneous and metamorphic rocks constitute ~37% of the surface lithology of the study area.

The volcanic rocks, including lava flows, tuffs, and volcaniclastic sediments of Cenozoic age, crop out extensively in the regions surrounding the Coso Range (Lanphere et al., 1975). This unit is mainly composed of Pleistocene, Pliocene, and Miocene

Table 1
Modal analyses of plutonic and volcanic rocks from the region

| Sample no. | 1 | 2 | 3 | 4 | 5 | 6 | 7 | 8 | 9 | 10[a] | 11[a] |
|---|---|---|---|---|---|---|---|---|---|---|---|
| Location | Argus range | Inyo mtns | El paso Mtns | El paso Mtns | Argus range | Spangler hills | Coso range | Coso range | Coso range | Spangler hills | Argus range |
| Minerals | Plutonic rocks | | | | | | Volcanic rocks | | | | |
| K-feldspar | 18.0 | 30.6 | 27.5 | 10.8 | 23.0 | 42.0 | 8.6 | 10.6 | 27.2 | – | 53.0 |
| Plagioclase | 55.6 | 35.1 | 36.8 | 56.1 | 42.0 | 21.0 | 62.7 | 55.2 | 38.1 | 28.0 | 27.0 |
| Quartz | 2.9 | 30.0 | 27.4 | 23.1 | 23.0 | 36.0 | – | – | 32.9 | 2.0 | 11.0 |
| Biotite | – | – | – | – | 6.0 | <1.0 | – | – | – | – | 4.0 |
| Hornblende | – | – | – | – | 4.0 | <1.0 | – | – | – | 63.0 | – |
| Olivine | – | – | – | – | – | – | 3.8 | 3.4 | – | – | – |
| Clinopyroxene | 10.9 | 0.8 | 3.3 | 4.5 | – | – | 17.0 | 22.3 | 1.1 | 3.0 | – |
| Calcite | 0.6 | 0.2 | 0.2 | 0.1 | – | – | 0.1 | 0.1 | – | – | – |
| Opaque minerals | 7.7 | 2.9 | 3.5 | 3.8 | 1.0 | <1.0 | 7.3 | 7.2 | 0.7 | 1.0 | 2.0 |
| Other minerals | 4.3 | 0.4 | 1.3 | 1.6 | 1.0 | <1.0 | 0.9 | 1.4 | <0.1 | 3.0 | 3.0 |

Modal analyses calculated from oxides. Dashes do not necessarily indicate that minerals are not present. Samples 1, 2, 3 and 4 are from Lee (1984), Table 3. Corresponding sample numbers are GR-129, GR-131, GR-149 and GR-151, respectively. Samples 5 and 6 are from Smith (1962), Table II. Corresponding sample numbers are GS-CG-1-60-6b and GS-CG-1-51-8b, respectively. Samples 7, 8 and 9 are from Duffield et al. (1980), Table 2. Corresponding sample numbers are 2, 9 and 10, respectively. Samples 10 and 11are from Smith (1962), Table I. Corresponding sample numbers are GS-CG-1-51-8a and GS-CG-1-60-4, respectively.

[a] Dike rocks.

volcanic rocks including rhyolites, andesites, basalts, olivine basalts, basaltic pyroclastic rocks. The volcanic rocks constitute 9% of the surface lithology.

Carbonate rocks constitute ~10% of the surface lithology and consist of a wide variety of Paleozoic and Mesozoic age rocks. There are Paleozoic and Mesozoic age limestone, dolomite, marble, calcareous shale and sandstone that outcrop along the flanks and throughout some parts of the mountains.

The Quaternary–Tertiary basin-fill deposits are a heterogeneous mixture of plutonic, volcanic and sedimentary rock detritus ranging from clay to boulder size. The mixture includes sand dune deposits, stream alluvium, stream-terrace deposits, coarse granitic debris flow, fan deposits, talus, slope wash, and glacial deposits. The unconsolidated materials deposited in fluvial and lacustrine environments of the valleys are relatively well sorted. The basin-fill deposits vary greatly in lithology, both vertically and areally. The percentage of silt and clay in the alluvium generally increases toward the playa-areas. Accordingly, the hydraulic properties of these deposits can differ greatly over short distances, both laterally and vertically. Thickness of basin-fill deposits ranges from zero at margins of valleys to as much as 610 m in IWV (Zbur, 1963) and more than 2440 m beneath Owens Lake (Hollett et al., 1991). The basin-fill deposits cover ~40% of the study area.

Quaternary playa deposits, are a relatively homogeneous deposit composed of mainly lenticular layers of interbedded salt deposits (evaporites), fine-grained sands, silts, clays, and lacustrine limestone. The evaporites are rich in sodium and calcium salts. Magnesium salts are extremely rare (Droste, 1961). Clay minerals primarily consist of illite and montmorillonite with lesser amounts of kaolinite and/or chlorite. The ratios of illite:montmorillonite:kaolinite and/or chlorite are 7:2:1 for Owens Lake, 4:5:1 for China Lake (Droste, 1961). The relative abundance of montmorillonite in China Lake sediments is related to volcanic eruptions in Quaternary time (Droste, 1961). The playa deposits cover ~5% of the study area.

## 3. Hydrology

Due to the modern arid climate, surface water is scarce in the area and mostly occurs in manmade reservoirs (e.g. Haiwee Reservoir and Lake Isabella). However, during the Quaternary period, valley floors were periodically occupied by a chain of lakes (Duffield and Smith, 1978). Present day, these locations are occupied by playas, known in different localities as 'salt lakes,' 'soda lakes,' 'alkali marshes,' 'dry lakes' or 'borax lakes' where the groundwater discharges by evapotranspiration (Lee, 1912; Fenneman, 1931; Dutcher and Moyle, 1973). The largest of the playas are Owens Lake, Searles Lake, and China Lake (Fig. 2). Near the playas, evapotranspiration constitutes the major flux of water out of the system. Such conditions can produce high chemical concentrations in evaporating groundwater, which can result in the precipitation of evaporate mineral deposits as salt crusts (Farnham et al., 2000). The most important crust-forming minerals are halite, natron, borax, thenardite, mirabilite, trona, burkeite, nahcolite, gaylussite, and pirssonite (Droste, 1961; Saint-Amand, 1986; Smith et al., 1971).

In a classic Basin and Range groundwater system, water flows from recharge areas in the mountains to discharge areas in adjacent valleys (Maxey, 1968). Groundwater occurs in two different porosity regimes: (1) fracture porosity found in the mountain watersheds; and (2) intergranular porosity found mostly in alluvial basin-fill aquifers. In the mountain watersheds, the water from precipitation at high altitudes percolates into a network of interconnecting fractures and faults existing within the igneous and metamorphic rocks, and under the influence of gravity moves toward points of lower head. In contrast, the groundwater in the alluvial aquifers moves through sediments that form a porous medium. Berenbrock and Schroeder (1994) estimate pre-development travel times of approximately 6000–13,000 years from the edges of the basin to the playa, which correspond to groundwater velocities of 0.21–0.76 m/year.

The alluvial basin-fill aquifer in IWV is defined by two components: (1) a shallow saline aquifer under the playa (<150 m deep); and (2) a deep (610 m), locally confined aquifer that extends throughout the valley (Dutcher and Moyle, 1973). The shallow aquifer consists of fine-grained lacustrine, alluvium, playa, and sand dune deposits perched on low permeability lacustrine clays near and around the playa lakes (Kunkel and Chase, 1969). The shallow

aquifer does not yield water freely to wells and contains water of poor quality (total dissolved solids (TDS) $> 1000\ mg\ l^{-1}$). The deep aquifer consists predominantly of high permeability fine to coarse sand and gravel, interbedded with silt and clay layers of lacustrine deposits, especially near the playas. The deep aquifer is currently being heavily pumped for its fresh water supply in IWV (Berenbrock and Martin, 1991).

## 4. Methodology

### 4.1. Database

Throughout the last 80 years, extensive hydrochemical data have been collected in the Indian Wells-Owens Valley area. The database used by this study is a compilation of most of these previously collected data (spring, surface, and well water data). This database was used for classification of waters into hydrochemical facies, also known as 'water types' or 'water groups'. The entire database consists of chemical analyses of 152 spring, 153 surface, and 1063 well samples; including temporal series (samples collected over a period of time at the same location). In the case of time series, more recent and/or the more complete sample data were included in the statistical analysis unless evaluation of temporal effects was desired. Database construction procedures are discussed in detail in Güler et al. (2002), where the sources of the data are also presented. Of the 39 hydrochemical variables in the compiled database, the variables Specific Conductance, pH, Ca, Mg, Na, K, Cl, $SO_4$, $HCO_3$, $SiO_2$, and F occur most often and were utilized in the statistical analyses.

### 4.2. Statistical clustering

Cluster analysis was used to determine if the samples can be grouped into statistically distinct hydrochemical groups that may be significant in the geologic context. A number of studies have used this technique to successfully classify water samples (Alther, 1979; Williams, 1982; Farnham et al., 2000; Alberto et al., 2001; Meng and Maynard, 2001). Comparisons based on multiple parameters from different samples are made and the samples grouped according to their 'similarity' to each other. The classification of samples according to their parameters is termed Q-mode classification. In this study, Q-mode HCA was used to classify the samples into distinct hydrochemical groups. Data treatment procedures and detailed explanation of the HCA clustering technique used by this study can be found in Güler et al. (2002).

### 4.3. Aqueous geochemical modeling

Inverse modeling calculations were performed using PHREEQC (Parkhurst and Appelo, 1999). PHREEQC was also used to calculate aqueous speciation and mineral saturation indices. The Geochemist's Workbench® was used to plot mineral stability diagrams (Bethke, 1994).

## 5. Results

### 5.1. Q-mode Hierarchical cluster analysis

A total of 1368 water samples from the Indian Wells-Owens Valley area and surrounding mountains are contained in the compiled database. Analysis of temporal series, as well as statistical analysis of the entire database suggested that relatively little change occurred in the water quality of samples with time (Güler, 2002; Güler et al., 2002). This indicates that spatial variability is the most important source of variation in the data. Therefore, removal of duplicate (in some cases multiple) water samples from the same location is warranted. Samples are given priority on the basis of completeness of data and date of collection. Removing the multiple samples reduced the total to 579.

The statistical software (Statistica; StatSoft, Inc., 1995) used in this study can only cluster a maximum of 300 samples, clearly a shortcoming given 579 water samples. Therefore, a two-step approach, pre-clustering and then clustering, was used. This methodology (pre-clustering and clustering) is currently used in several clustering algorithms (e.g. SAS/STAT release 6.03; SAS Institute, Inc., 1988) to cluster samples.

First, 579 water samples were subdivided into four major categories consisting of: (1) spring waters

(SP = 118 samples); (2) surface waters (SU = 137 samples); (3) shallow well waters (WS = 264 samples); and (4) deep well waters (WD = 60 samples). Then, each data set was log-transformed and standardized (to zero mean and unit variance) to avoid misclassifications arising from the different orders of magnitude of both parameter value and the variance of the parameters analyzed (Johnson and Wichern, 1992). Finally, each data set was separately pre-clustered by using the Q-mode HCA technique.

Pre-clustering of the four data sets resulted in a total of 32 water subgroups (9 spring water, 7 surface water, 10 shallow well water, and 6 deep well water). Spring water subgroup 6 (SP6) was composed of one sample, which had an abnormally low (erroneous) silica value, and was excluded from further analysis. For the remaining 31 subgroups, mean values for each of the 11 parameters (Specific Conductance, pH, Ca, Mg, Na, K, Cl, $SO_4$, $HCO_3$, $SiO_2$, and F) were calculated (Table 2). Finally, this reduced data matrix (11 by 31) was clustered again, resulting in

Table 2
Subgroups (determined from HCA) that compose the five principal water groups and their mean water chemistry

| Group | Sub-group | N[a] | pH | S. Cond. | Ca | Mg | Na | K | Cl | $SO_4$ | $HCO_3$ | $SiO_2$ | F | TDS |
|---|---|---|---|---|---|---|---|---|---|---|---|---|---|---|
| 1 | SU7 | 11 | 7.2 | 48.0 | 1.6 | 0.2 | 0.8 | 0.7 | 0.7 | 1.8 | 6.2 | – | 0.0 | 8.9 |
| | SU6 | 30 | 7.1 | 41.0 | 3.3 | 0.6 | 4.3 | 0.6 | 0.6 | 0.8 | 25.1 | 20.0 | 0.1 | 42.9 |
| | SU5 | 25 | 7.7 | 111.7 | 11.9 | 1.5 | 10.5 | 1.3 | 2.4 | 3.0 | 69.7 | 23.7 | 0.3 | 89.5 |
| | SP9 | 15 | 7.2 | 92.5 | 11.6 | 1.2 | 12.1 | 0.9 | 1.2 | 0.8 | 70.6 | 22.2 | 0.8 | 70.7 |
| 2 | WD4 | 7 | 9.7 | 547.0 | 2.1 | 0.2 | 96.1 | 1.3 | 10.5 | 19.2 | 182.1 | 28.1 | 0.4 | 248.9 |
| | WS1 | 30 | 8.3 | 490.0 | 10.6 | 2.5 | 97.9 | 4.5 | 51.2 | 19.1 | 179.5 | 35.4 | 0.8 | 317.6 |
| | WD5 | 12 | 8.5 | 838.0 | 7.3 | 1.1 | 171.0 | 2.9 | 63.1 | 35.6 | 309.7 | 36.2 | 3.2 | 475.3 |
| | SU1 | 20 | 8.1 | 310.3 | 38.3 | 5.3 | 22.7 | 2.1 | 7.0 | 20.0 | 177.7 | 34.8 | 0.7 | 219.7 |
| | SP8 | 8 | 8.0 | 272.6 | 22.4 | 1.8 | 31.0 | 1.0 | 5.6 | 19.7 | 124.4 | 32.3 | 2.6 | 205.2 |
| | SP7 | 18 | 7.1 | 397.8 | 42.3 | 8.6 | 29.3 | 2.8 | 15.2 | 38.0 | 177.5 | 37.3 | 0.6 | 308.1 |
| | WS2 | 55 | 7.9 | 642.0 | 34.0 | 7.1 | 88.0 | 4.0 | 82.6 | 65.6 | 145.4 | 32.7 | 0.9 | 385.1 |
| | WD6 | 20 | 7.9 | 481.0 | 31.6 | 7.7 | 66.2 | 4.0 | 36.0 | 62.9 | 167.0 | 29.8 | 0.6 | 322.4 |
| | SU2 | 31 | 8.0 | 629.2 | 67.8 | 19.5 | 44.8 | 4.7 | 19.3 | 80.4 | 294.2 | 32.8 | 0.8 | 417.2 |
| | SP5 | 28 | 7.9 | 550.2 | 63.0 | 15.2 | 32.9 | 3.2 | 25.6 | 68.7 | 220.6 | 25.1 | 0.3 | 344.2 |
| 3 | WS3 | 36 | 7.6 | 2304.0 | 138.0 | 40.1 | 286.9 | 14.8 | 460.8 | 356.8 | 162.2 | 58.7 | 0.9 | 1396.9 |
| | WS4 | 45 | 7.6 | 1189.0 | 59.3 | 26.3 | 168.3 | 10.2 | 122.0 | 139.0 | 371.1 | 40.4 | 0.8 | 748.7 |
| | SU4 | 3 | 8.9 | 1276.7 | 30.1 | 40.6 | 201.9 | 17.4 | 158.2 | 13.7 | 487.3 | – | 0.0 | 705.6 |
| | SP4 | 27 | 7.7 | 855.1 | 95.9 | 29.1 | 70.8 | 3.9 | 46.3 | 211.9 | 274.8 | 36.4 | 1.2 | 646.2 |
| | WS8 | 17 | 8.2 | 1721.0 | 12.2 | 19.3 | 363.2 | 21.2 | 197.5 | 48.7 | 696.8 | 58.2 | 3.5 | 1043.5 |
| | WD2 | 13 | 8.4 | 2908.0 | 39.0 | 40.6 | 572.2 | 13.9 | 162.5 | 105.3 | 1398.6 | 33.7 | 2.0 | 1668.4 |
| | SU3 | 17 | 8.4 | 1524.1 | 75.7 | 55.7 | 180.3 | 15.5 | 113.6 | 203.3 | 489.3 | 34.7 | 1.8 | 925.2 |
| | SP1 | 10 | 7.9 | 1657.0 | 54.0 | 32.0 | 261.2 | 22.0 | 224.2 | 175.5 | 453.4 | 46.1 | 2.2 | 1063.5 |
| 4 | WS6 | 15 | 7.1 | 6968.0 | 342.9 | 78.1 | 1129.5 | 39.3 | 2243.3 | 440.0 | 112.2 | 8.5 | 1.8 | 4367.7 |
| | WD1 | 2 | 7.9 | 11200.0 | 502.0 | 25.4 | 1755.0 | 24.0 | 3615.0 | 223.2 | 19.5 | – | 2.3 | 6157.4 |
| | WS5 | 27 | 7.7 | 8762.0 | 167.3 | 157.9 | 1878.2 | 68.7 | 2189.3 | 1767.6 | 403.4 | 57.5 | 1.6 | 6538.5 |
| | SP2 | 7 | 7.0 | 6264.2 | 70.7 | 75.1 | 1287.0 | 77.6 | 1165.7 | 433.7 | 1541.1 | 101.8 | 1.7 | 4347.9 |
| | WS7 | 25 | 8.7 | 6784.0 | 9.7 | 14.7 | 1676.1 | 32.6 | 1680.2 | 488.1 | 996.8 | 20.6 | 3.6 | 4475.9 |
| | SP3 | 4 | 9.1 | 4160.0 | 4.4 | 3.4 | 967.8 | 77.3 | 464.5 | 336.3 | 1122.3 | 50.5 | – | 3206.3 |
| 5 | WS10 | 7 | 9.5 | 71800.0 | 4.2 | 1.8 | 37300.0 | 1140.0 | 41442.9 | 7671.4 | 9379.6 | 31.4 | 11.7 | 96254.8 |
| | WS9 | 7 | 8.4 | 117657.0 | 252.3 | 265.6 | 55100.0 | 825.6 | 72357.1 | 5849.9 | 6745.1 | 12.5 | 29.2 | 147444.4 |
| | WD3 | 6 | 8.9 | 34440.0 | 52.7 | 55.8 | 10536.7 | 87.0 | 10046.7 | 3008.0 | 12580.7 | 46.5 | 40.8 | 30164.4 |

SU, Surface water (7 subgroups); SP, Spring water (8 subgroups); WS, Shallow Well water (10 subgroups); WD, Deep Well water (6 subgroups). pH (standard units), Specific Conductance (μSiemens $cm^{-1}$), and mean concentrations and TDS (total dissolved solids) (mg $l^{-1}$).

[a] Number of samples within respective subgroups.

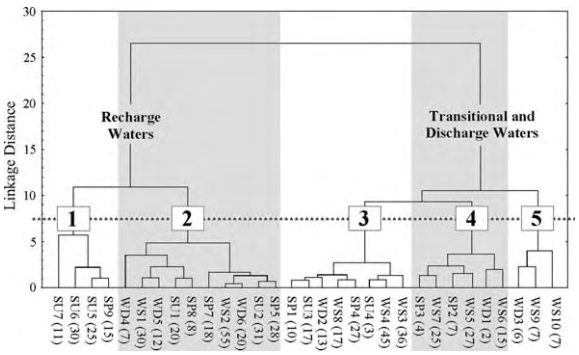


Fig. 3. Dendogram of Q-mode hierarchical cluster analysis (HCA) showing associations between samples from different parts of the hydrologic system. Line of asterisks defines "phenon line", which is chosen by analyst to select number of groups or subgroups. X-axis shows subgroups of samples with number of samples in parentheses, definitions are in Table 2.

a dendogram showing associations between waters from different parts of the hydrologic system (Fig. 3). Applying this two-step clustering technique, the waters from the area were classified into five principal hydrochemical facies or water types based on the multivariate statistics. These are: Group-1 ($Ca–Na–HCO_3$ water); Group-2 ($Na–Ca–HCO_3$ water); Group-3 ($Na–HCO_3–Cl$ water); Group-4 (Na–Cl water); and Group-5 (more concentrated Na–Cl water).

Table 3 shows the group means for each of the parameters produced by the HCA analysis. These values reveal some trends between the principal groups. TDS seems to be a major distinguishing factor with concentrations increasing in all major-ions following the order: Group-1, Group-2, Group-3, Group-4, and Group-5 (Table 3). Group-1 samples have extremely low TDS values (average is $\sim 67\ mg\ l^{-1}$), up to Group-5 samples that have the highest TDS values (average is $\sim 94{,}000\ mg\ l^{-1}$).

Although statistical analysis of data can be useful, statistics have little meaning unless the underlying physical or chemical processes are known and the numerical relationships can be related to natural processes. The relationship between the statistically-defined clusters of samples and geographic location was tested by plotting group values for each sample on a shaded-relief site map using ArcView GIS software (ESRI, 1996) (Fig. 4). The five groups are separated geographically, as well as physiographically with good correspondence between spatial locations and the statistical groups as determined by the HCA. Samples that belong to the same group are located in close proximity to one another suggesting the same processes and/or flowpaths for these group of samples. The high degree of spatial and statistical coherence suggests that the changes between the principal hydrochemical facies define the hydrochemical evolution of water in the region, but this hypothesis requires further testing.

The majority of samples are located in IWV and the adjacent Sierra Nevada. Discussion of results will mainly relate to these data, although similar trends are evident in the adjacent basin and ranges. The TDS of water samples increase as the water moves eastward from the Sierran recharge areas to the discharge areas near and around the playas. The five principal hydrochemical facies are plotted on a Piper diagram (Piper, 1944) to illustrate chemical differences between the groups and the geochemical changes along the topographic flowpaths (Fig. 5). Groundwater

Table 3
Mean parameter values for the precipitation (snow) and five principal water groups used in inverse modeling calculations

| Group | N[a] | pH | Ca | Mg | Na | K | Cl | $SO_4$ | $HCO_3$ | $SiO_2$ | TDS |
|---|---|---|---|---|---|---|---|---|---|---|---|
| Snow[b] | 18 | 5.9 | 0.8 | 0.2 | 0.4 | 0.4 | 0.5 | 1.1 | 3.6 | 0.2 | 5.6 |
| 1 | 81 | 7.3 | 7.3 | 0.9 | 7.2 | 0.9 | 1.3 | 1.6 | 44.7 | 21.5 | 67.5 |
| 2 | 229 | 8.0 | 37.1 | 8.5 | 67.1 | 3.6 | 41.1 | 50.9 | 195.4 | 32.5 | 355.7 |
| 3 | 168 | 7.9 | 76.5 | 33.7 | 236.4 | 12.9 | 199.1 | 192.1 | 442.3 | 42.7 | 1018.0 |
| 4 | 80 | 7.9 | 142.8 | 79.9 | 1574.3 | 52.0 | 1900.2 | 891.9 | 660.1 | 41.2 | 5133.4 |
| 5 | 20 | 8.9 | 105.6 | 110.3 | 35501.0 | 714.0 | 42844.0 | 5634.9 | 9417.9 | 33.7 | 93588.4 |

pH (standard units) and mean concentrations and TDS (total dissolved solids) ($mg\ l^{-1}$).
[a] Number of samples within respective principal groups.
[b] Snow (Sierra Nevada eastside), 1957–59, Feth et al. (1964b), Tables 1 and 2.

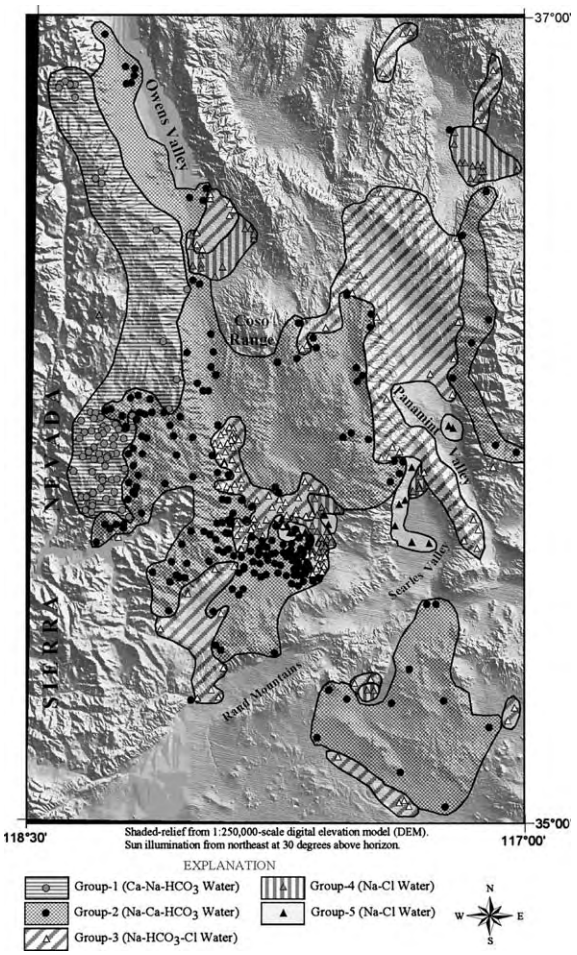


Fig. 4. Spatial distribution of the statistically-defined five principal water groups in the study area. Symbols indicate sample locations.

in the recharge area evolves from a dilute Ca–Na–$HCO_3$ water (1: average TDS is ~67 mg $l^{-1}$) to a fresh Na–Ca–$HCO_3$ water (2: average TDS is ~356 mg $l^{-1}$) to a more concentrated Na–$HCO_3$–Cl water (3: average TDS is ~1018 mg $l^{-1}$) to a brackish Na–Cl water (4: average TDS is ~5133 mg $l^{-1}$) to a Na–Cl brine (5: average TDS is ~94,000 mg $l^{-1}$, with TDS locally as high as 370,000 mg $l^{-1}$) along the topographic flowpath (Table 3 and Figs. 4 and 5). Overall, the waters from the area can be classified as recharge area waters (Group-1 and Group-2), transition zone waters (Group-3) and discharge area waters (Group-4 and Group-5).

Plotting the principal hydrochemical facies on the site map shows that Group-1 waters, composed of surface water subgroups 5, 6 and 7 (SU5, SU6, SU7) and spring water subgroup 9 (SP9), are all located in the recharge areas of the high Sierra Nevada. In fact, most of the samples composing Group-1 are above 2000 m. In Fig. 3, the clustering of SP9 (spring) samples with the SU5, SU6 and SU7 (surface water) samples reflect the short groundwater flowpaths for the low TDS (dilute) spring waters. Recharge to these springs probably occur via fault and/or fracture controlled shallow groundwater flowpaths. Similar values for surface and spring water temperature support local recharge to these springs. The importance of local fractures and faults on surface and groundwater flow in the Sierra Nevada has been noted (Howard et al., 1997a,b).

Group-2 samples are mostly located below 2000 m in the Sierra Nevada and other mountain ranges. These areas provide the majority of recharge to the basin-fill aquifers (Maxey, 1968). Group-3 samples are usually located on the basin floors, and are spatially between Group-2 and Group-4 samples as expected since they represent the continued evolution of water chemistry between recharge and discharge zones. Group-4 samples are found in the discharge areas (playas) and have the second highest TDS concentration (average TDS is ~5133 mg $l^{-1}$) of all the groups. Group-5 waters have the highest TDS concentrations and coincide with the playa or nearby discharge area (Fig. 4).

### 5.2. Hydrochemical evolution

A more detailed hydrochemical evolution pattern is displayed in Fig. 6. The Cl, Na, K and $SO_4$ concentrations show systematic increases with TDS. The $SiO_2$, Ca and Mg concentrations increase until they reach mineral saturation, which is reflected in the slower increase or even decrease in concentration with increasing TDS as these solutes precipitate along the groundwater flowpaths. The plot shows three phases in the hydrochemical evolution. The first phase is the evolution between Groups 1 and 2, where the TDS increases significantly, as do all the dissolved parameters. The second phase includes the changes between Groups 2 to 3 with the pH remaining constant or slightly decreasing along the flowpath as TDS

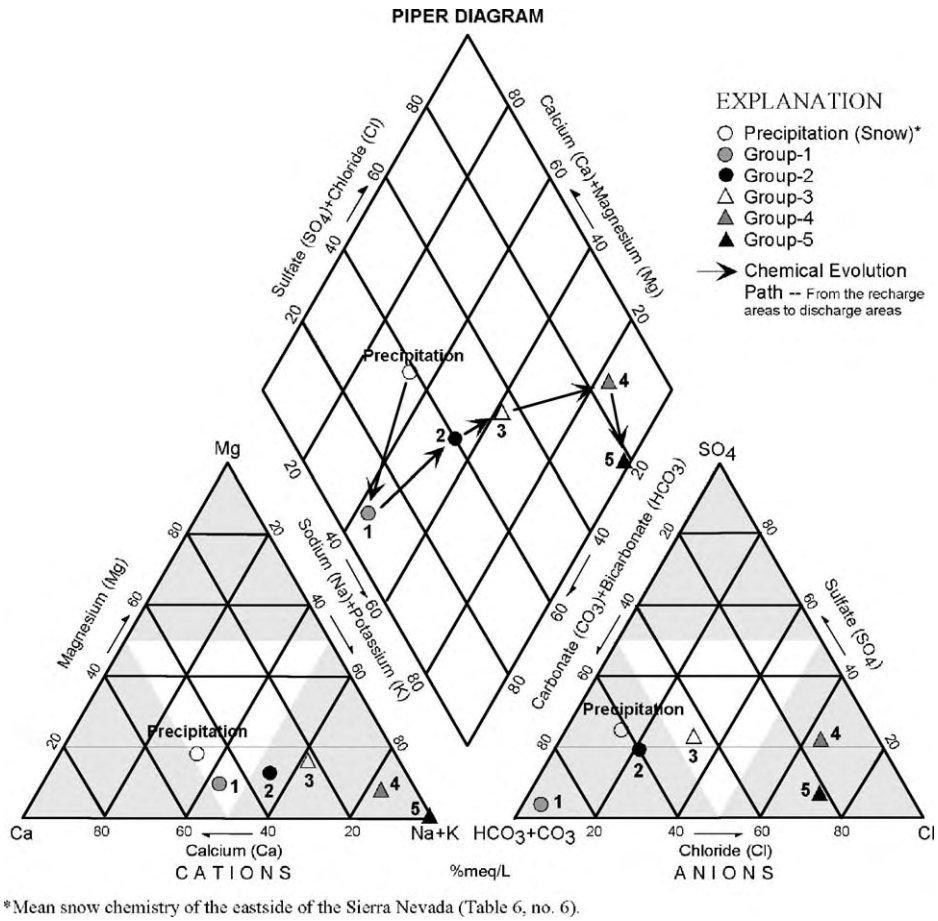


Fig. 5. Piper diagram of the chemical evolution of groundwater in the study area (starting with precipitation (snow) and ending with playa-area waters). Total dissolved solids (TDS) concentration increases with increasing group number.

slowly increases with some parameters (Ca, Mg and $SiO_2$) remaining constant. The third phase is the rapid increase in TDS between Group-3 and Groups 4 and 5.

These trends indicate that the reactions during the short flow times in the fractured rock aquifer in the Sierra Nevada are important in the initial hydrochemical evolution (Precipitation to Group-1 or Group-1 to Group-2). The hydrochemical evolution during the flow through the porous media basin aquifers continues, with an increase in TDS, but not to the degree as the early reactions. The final phase of hydrochemical evolution occurs near the playa where a very large increase in TDS are linked to increases in Na, $SO_4$, $HCO_3$ and Cl, suggesting that dissolution of salts are a significant control during this stage.

### 5.3. Geochemical modeling

#### 5.3.1. Saturation data

Saturation indices are used to evaluate the degree of equilibrium between water and minerals. Changes in saturation state are useful to distinguish different stages of hydrochemical evolution and help identify which geochemical reactions are important in controlling water chemistry. The saturation indices for precipitation (snow) and the water groups are compiled in Table 4.

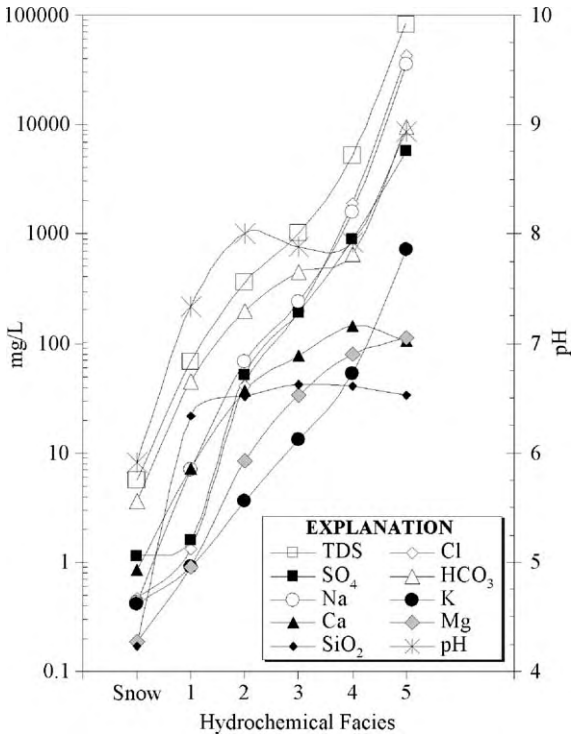


Fig. 6. Detailed evolution of hydrochemical facies from precipitation (snow) to Group-5 in the study area. Note that pH values are displayed in right-hand y-axis.

The results of saturation calculations show that all the facies (except Group-1) are supersaturated with respect to kaolinite and smectite (Ca, Mg–saponite) (Table 4). Halite and gypsum are undersaturated in all facies suggesting that their soluble component Na, Cl, Ca and $SO_4$ concentrations are not limited by mineral equilibrium. In contrast, calcite, K-feldspar, hornblende and plagioclase reach saturation by Group-2 as groundwater chemistry evolves along the groundwater flowpaths. The groundwater saturation indices for quartz and amorphous silica also reach a constant saturated value in the facies three samples. The primary minerals biotite and forsterite are always undersaturated indicating that they will dissolve along the flowpath. When groundwater reach the playa areas, evapotranspiration concentrates the solutes and TDS increases rapidly. The samples from the playa (facies 5) are supersaturated with respect to several salt minerals, such as gaylussite and pirssonite (Table 4), which have been reported in salt crusts of the playas (Droste, 1961; Saint-Amand, 1986; Smith et al., 1971).

The pattern of saturation indices and TDS increasing with decreasing elevation of sample localities appears to define the topographic flowpath of Sierra Nevada recharge moving towards

Table 4
Saturation indices of the snow and five principal water groups with respect to various mineral phases. Phases and thermodynamic data are from PHREEQC and accompanying databases (Parkhurst and Appelo, 1999)

| Phases | Stoichiometry | Snow[a] | Group-1 | Group-2 | Group-3 | Group-4 | Group-5 |
|---|---|---|---|---|---|---|---|
| Albite[1] | $NaAlSi_3O_8$ | −10.7 | −1.8 | −0.6 | 0.3 | 0.8 | 2.4 |
| Amorphous silica[1] | $SiO_2(a)$ | −2.7 | −0.6 | −0.5 | −0.4 | −0.4 | −0.4 |
| Anorthite[1] | $CaAl_2Si_2O_8$ | −12.9 | −4.2 | −2.9 | −2.5 | −2.6 | −2.6 |
| Biotite[2] | $KMg_3AlSi_3O_{10}(OH)_2$ | −56.1 | −36.3 | −27.4 | −25.8 | −24.2 | −16.6 |
| Calcite[1] | $CaCO_3$ | −5.1 | −1.6 | 0.4 | 0.8 | 1.1 | 2.3 |
| Chalcedony[1] | $SiO_2$ | −1.8 | 0.3 | 0.3 | 0.5 | 0.4 | 0.5 |
| Forsterite[3] | $Mg_2SiO_4$ | −23.0 | −13.0 | −7.4 | −6.8 | −5.9 | −1.6 |
| Gaylussite[4] | $CaNa_2(CO_3)_2{:}5H_2O$ | −21.8 | −13.5 | −8.5 | −6.8 | −4.9 | 0.6 |
| Gypsum[1] | $CaSO_4{:}2H_2O$ | −5.1 | −4.1 | −2.1 | −1.5 | −0.9 | −1.2 |
| Halite[2] | NaCl | −11.2 | −9.5 | −7.1 | −5.9 | −4.2 | −1.6 |
| Hornblende[3] | $Ca_2Mg_5Si_8O_{22}(OH)_2$ | −58.2 | −14.7 | 3.6 | 5.7 | 8.0 | 22.1 |
| Kaolinite[1] | $Al_2Si_2O_5(OH)_4$ | 0.2 | 4.4 | 2.9 | 3.3 | 2.8 | 1.0 |
| K-feldspar[1] | $KAlSi_3O_8$ | −8.1 | −0.2 | 0.5 | 1.4 | 1.6 | 3.0 |
| Nahcolite[4] | $NaHCO_3$ | −8.6 | −6.3 | −4.9 | −4.0 | −3.1 | −1.2 |
| Pirssonite[4] | $Na_2Ca(CO_3)_2{:}2H_2O$ | −21.9 | −13.7 | −8.6 | −7.0 | −5.0 | 0.6 |
| Plagioclase[5] | $Na_{0.62}Ca_{0.38}Al_{1.38}Si_{2.62}O_8$ | −8.2 | −0.1 | 0.3 | 1.0 | 0.9 | 1.8 |
| Quartz[1] | $SiO_2$ | −1.3 | 0.7 | 0.8 | 0.9 | 0.8 | 0.9 |
| Saponite-Ca[6] | $Ca_{0.165}Mg_3Al_{0.33}Si_{3.67}O_{10}(OH)_2$ | −22.5 | −3.9 | 3.2 | 4.4 | 5.0 | 11.1 |
| Saponite-Mg[6] | $Mg_{3.165}Al_{0.33}Si_{3.67}O_{10}(OH)_2$ | −22.5 | −4.0 | 3.2 | 4.4 | 5.0 | 11.2 |

Saturation index (SI) = Log [Ion Activity Product]/$K_T$, where $K_T$ = equilibrium constant at temperature $T$. Saturation indices were calculated by the computer program PHREEQC (Version 2.0) (Parkhurst and Appelo, 1999). Sources of thermodynamic data: 1 = PHREEQC, 2 = MINTEQ, 3 = WATEQ4F, 4 = LLNL, 5 = Calculated, 6 = Geochemist's Workbench (Bethke, 1994).

[a] Mean snow chemistry of the eastside of the Sierra Nevada (Table 6, no. 6).

Table 5
Summary of mass transfer for selected inverse geochemical models. Phases and thermodynamic data are from PHREEQC and accompanying databases (Parkhurst and Appelo, 1999)

| Phases | Flowpath and model number | | | | | | | | |
|---|---|---|---|---|---|---|---|---|---|
| | Precipitation to group-1 | | Group-1–Group-2 | | Group-2–Group-3 | | Group-3–Group-4 | Group-4–Group-5 | |
| | Model 1 | | Model 2 | | Model 3 | | Model 4 | Model 5 | |
| Amorphous silica | −2.49E-04 | −2.66E−04 | −3.54E-03 | −3.98E-03 | – | – | – | – | – |
| Biotite | 1.15E-05 | – | 6.81E-05 | – | 2.40E-04 | 2.40E-04 | 9.23E-04 | 1.85E-02 | 1.85E-02 |
| Calcite | – | – | -8.74E-04 | -9.97E-04 | -4.32E-04 | -4.32E-04 | -6.51E-03 | – | – |
| $CO_2$(g) | 5.68E-04 | 5.68E-04 | 3.68E-03 | 3.80E-03 | 5.21E-03 | 5.21E-03 | 1.19E-02 | – | – |
| Forsterite | – | 1.73E-05 | 5.11E-05 | – | 2.12E-03 | 2.12E-03 | 7.44E-03 | – | – |
| Hornblende | – | – | – | 6.13E-05 | – | – | – | – | – |
| K-feldspar | 3.75E-06 | 1.53E-05 | – | 6.81E-05 | – | – | – | – | – |
| Plagioclase | 4.63E-04 | 4.63E-04 | 2.85E-03 | 2.85E-03 | – | – | – | – | – |
| Kaolinite | −3.27E-04 | −3.27E-04 | −2.00E-03 | −2.00E-03 | – | – | – | −7.42E-03 | −7.42E-03 |
| Saponite-Ca | – | – | – | – | – | −7.27E-04 | – | – | −1.11E-02 |
| Saponite-Mg | – | – | – | – | −7.27E-04 | – | −2.80E-03 | −1.11E-02 | – |
| Gypsum | 3.86E-06 | 3.86E-06 | 5.15E-04 | 5.15E-04 | 1.40E-03 | 1.49E-03 | 7.90E-03 | 5.55E-02 | 5.55E-02 |
| Halite | 2.44E-05 | 2.44E-05 | 1.13E-03 | 1.13E-03 | 4.48E-03 | 4.24E-03 | 4.78E-02 | 1.28E + 00 | 1.28E + 00 |
| Nahcolite | – | – | – | – | – | – | – | 1.35E-01 | 1.35E-01 |
| Ca-ion exchange | – | – | – | – | – | – | – | −5.61E-02 | −5.43E-02 |
| Na-ion exchange | – | – | – | – | 3.27E-03 | 3.50E-03 | 1.38E-02 | 1.50E-01 | 1.50E-01 |
| Mg-ion exchange | – | – | – | – | −1.63E-03 | −1.75E-03 | −6.89E-03 | −1.86E-02 | −2.05E-02 |

Values in moles per kilogram $H_2O$ (positive values indicate dissolution and negative values indicate precipitation). Dashes indicate phase not used in model.

the playa-areas. Fig. 6 shows that dissolved $SiO_2$, Ca and Mg equilibrium with aquifer minerals (Table 5) are likely an important control on the hydrochemical evolution.

*5.3.2. Mineral stability diagrams*

Another approach to test the proposed hydrochemical evolution is the use of mineral stability diagrams (Drever, 1988). Fig. 7 shows four mineral stability diagrams for the $MgO–CaO–Al_2O_3–H_2O–SiO_2$ system (Fig. 7a), the $CaO–Na_2O–Al_2O_3–H_2O–SiO_2$ system (Fig. 7b), the $Na_2O–Al_2O_3–H_2O–SiO_2$ system (Fig. 7c), and the $K_2O–Al_2O_3–H_2O–SiO_2$ system (Fig. 7d). The values from 579 samples representing each of the five principle water groups are plotted on the diagrams to help define the reactions that control the water chemistry. The majority of water samples from Groups 1 and 2 plot in the kaolinite field

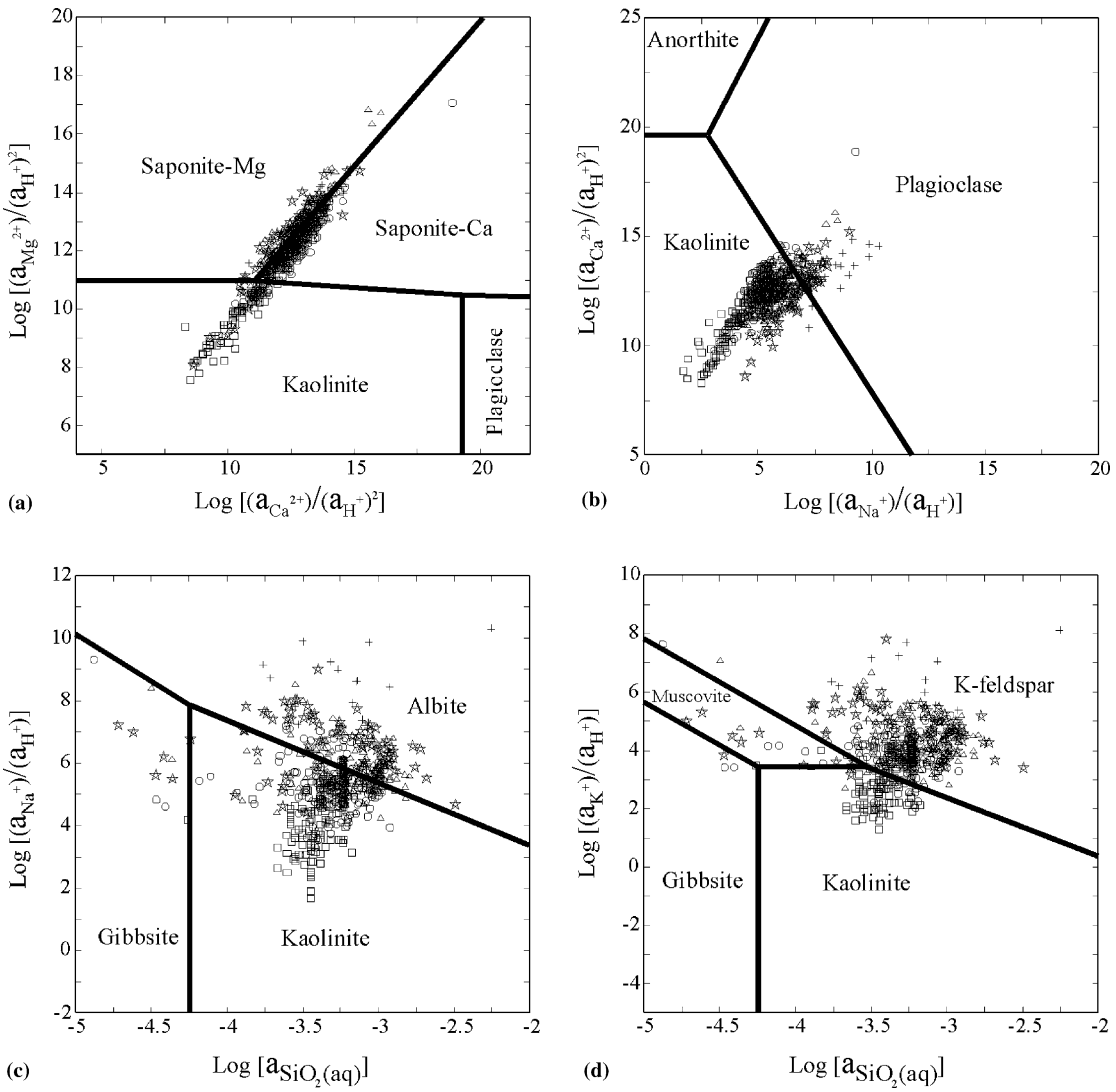


Fig. 7. Mineral stability diagrams for $MgO-CaO-Na_2O-K_2O-Al_2O_3-H_2O-SiO_2$ systems at 25°C and 1 atmosphere (1.013 bars) total pressure. Symbols show sample values from different water groups. Box = Group-1, circle = Group-2, triangle = Group-3, star = Group-4 and plus = Group-5.

or along the Ca–smectite and Mg–smectite boundary suggesting that equilibrium with kaolinite or smectite is an important process controlling water chemistry (see Fig. 7a). Smectitic clay is a major component in area lakebeds (Bischoff et al., 1997). In contrast, some of the higher TDS samples extend into the plagioclase, albite and K-feldspar stability fields suggesting equilibrium between clays and primary minerals is likely not the main processes controlling the water chemistry (Fig 7b–d). Lastly, the maximum dissolved silica concentrations do not exceed $10^{-2.75}$ mole/kg, suggesting that dissolved silica is ultimately controlled by equilibrium with an amorphous silica phase rather than quartz or chalcedony. These observations help to further constrain the hydrochemical evolution.

*5.3.3. Inverse modeling*

Inverse modeling is often used for interpreting geochemical processes that account for the hydrochemical evolution of groundwater (Plummer et al., 1983, 1992, 1994). This mass balance approach uses two water analyses represent starting (initial) and ending (final) water compositions along a flowpath to calculate the moles of minerals and gases that must enter or leave solution to account for the differences in composition (Parkhurst et al., 1980). In geochemical modeling, either forward or inverse, soundness of results are dependent upon valid conceptualization of the system, validity of basic concepts and principles, accuracy of input data, and level of understanding of the geochemical processes. We use the information from the lithology, general hydrochemical evolution patterns, saturation indices and mineral stability diagrams to constrain the inverse models.

Inverse models for the observed changes between precipitation and the five principal groups were formulated. The average chemical parameter values for the statistical clusters were used to represent 'initial' and 'final' waters along a groundwater flowpath (Table 3). The inverse models were formulated so that primary mineral phases including K-feldspar, hornblende, forsterite, plagioclase and biotite are constrained to dissolve until they reach saturation, and calcite, amorphous silica, kaolinite and smectite were set to precipitate once they reached saturation. Halite and gypsum are included as sources of Cl and $SO_4$, respectively, and ion exchange, which has been cited as an important process in groundwater evolution in the area was included in models for Groups 3, 4 and 5. Carbon dioxide gas was assumed to be available throughout the flowpath. Usually a source of $CO_2$ would not be available in the groundwater out of contact with the atmosphere, however, IWV is a geothermal area. As the general geochemical evolution showed the pH decreases slightly along the groundwater flowpath (Groups 3 and 4) indicating a continuous source of $CO_2$ in addition to the atmosphere. Finally, models for Group-5 included playa salts such as mirabilite, nahcolite, gaylussite, pirssonite and thenardite. Table 5 shows selected results of the inverse modeling. The models in Table 5 were selected from all the possible models based on the statistical measures calculated by PHREEQC (sum of residuals and maximum fractional error) and to represent different possible combinations of reactants and products that can account for the change in water chemistry. Except for model 4, there were two equally valid, but different models for each hydrochemical evolution step. One of the most valuable aspects of using the mean values from statistical clusters is that we maximize the 'uniqueness' of the inverse modeling solution by producing the minimum number of models, rather than the more usual result of producing many non-unique models. Thus, for model 1 the difference between the two possible models is the dissolution of biotite or forsterite. In reality, both minerals undergo dissolution, but the modeling software produces only models that use one of the two phases.

*5.3.3.1. Evolution of precipitation (Snow) to Group-1 Waters*. The extremely low TDS of the Group-1 waters suggests that the surface water does not remain in contact with the surface bedrock long enough for significant dissolution to occur. Dilute waters of Group-1 are undersaturated with respect to calcite (Table 4), indicating waters at the earliest stages of evolution. This also suggests relatively short flowpaths for this group of waters. In the high Sierra Nevada, where Group-1 waters dominate, vegetation is usually sparse with scattered coniferous trees and shrubs, thus, the effect of vegetation on weathering and consequently on water chemistry is assumed to be minimal in the area.

Average snow chemistry of the eastern Sierra Nevada (Table 6, no. 6) was used as the starting

Table 6
Precipitation chemistry of the Sierra Nevada region

| | 1[a] | 2[a] | 3[b] | 4[b] | 5[b] | 6[b] | 7[a] | 8[b] | 9[a] |
|---|---|---|---|---|---|---|---|---|---|
| pH | 5.34 | 5.10 | – | 5.86 | 5.82 | 5.92 | 4.88 | 4.87 | 5.19 |
| Cond. | 3.30 | 7.70 | – | 6.37 | 7.64 | 8.98 | 18.30 | 18.53 | 4.90 |
| Ca | 0.026 | 0.134 | 0.40 | 0.15 | 0.22 | 0.84 | 0.481 | 0.415 | 0.080 |
| Mg | 0.007 | 0.015 | 0.17 | 0.20 | 0.03 | 0.19 | 0.058 | 0.056 | 0.023 |
| Na | 0.030 | 0.085 | 0.46 | 0.49 | 0.46 | 0.43 | 0.354 | 0.463 | 0.092 |
| K | 0.027 | 0.059 | 0.32 | 0.32 | 0.25 | 0.41 | 0.149 | 0.129 | 0.027 |
| Cl | 0.099 | 0.184 | 0.50 | 0.54 | 0.48 | 0.47 | 0.323 | 0.250 | 0.223 |
| $SO_4$ | 0.096 | 0.442 | 0.95 | 1.06 | 0.63 | 1.14 | 1.849 | 1.862 | 0.399 |
| $HCO_3$ | – | – | 2.88 | 3.31 | 2.00 | 3.59 | – | – | – |
| $NO_3$ | 0.143 | 0.893 | 0.07 | 0.008 | 0.133 | 0.15 | 2.653 | 2.665 | 0.360 |
| $NH_4$ | 0.031 | 0.375 | – | 0.20 | 0.00 | 0.00 | 0.997 | 0.925 | 0.132 |
| $SiO_2$ | – | – | 0.16 | 0.18 | 0.14 | 0.17 | – | – | – |

(1). Winter snowfall (Sierra Nevada westside), 1985–88, $N = 834$, Williams and Melack (1991a), Table 4. (2). Autumn snowfall (Sierra Nevada westside), 1985–87, $N = 12$, Williams and Melack (1991a), Table 10. (3). Snow (Sierra Nevada), $N_{min} = 42$, $N_{max} = 79$, Feth et al. (1964a), Table 3. (4). Snow (Sierra Nevada westside), 1957–59, $N_{min} = 20$, $N_{max} = 29$, Feth et al. (1964b), Table 1 and 2. (5). Snow (Sierra Nevada crest), 1957–59, $N_{min} = 9$, $N_{max} = 31$, Feth et al. (1964b), Table 1 and 2. (6). Snow (Sierra Nevada eastside), 1957–59, $N_{min} = 10$, $N_{max} = 18$; Feth et al. (1964b), Table 1 and 2. (7). Rain (Sierra Nevada westside), 1985–87, $N = 23$, Williams and Melack (1991a), Table 10 (8). Spring Rain (Sierra Nevada westside), April–June 1987, $N = 7$, Williams and Melack (1991b), Table 1. (9). Wet deposition (Sierra Nevada westside), 1981–84, $N =$ unknown, Stohlgren and Parsons (1987), Table 1.

[a] Volume-weighted mean concentrations (mg $l^{-1}$), pH (standard units), and Conductance (μSiemens $cm^{-1}$).

[b] Mean concentrations (mg $l^{-1}$), pH (standard units), and Conductance (μSiemens $cm^{-1}$).

solution for inverse geochemical modeling calculations. Snow chemistry of the eastern Sierra Nevada is slightly acidic (pH 5.9) and is dominated by calcium and bicarbonate (Table 6). Calcium, potassium, and sulfate are noticeably enriched relative to precipitation from the western Sierra Nevada suggesting the importance of locally derived windblown dust (from playas) on the precipitation chemistry of the area.

Dilute snowmelt runoff (dominated by Ca and $HCO_3$ ions) is an active agent in chemical weathering reactions that are occurring in the alpine watersheds of the Sierra Nevada. Even though the area is underlain by granitic bedrock with poorly developed soils, interactions between snowmelt runoff and soils and/or rocks is important to the hydrochemistry of the alpine watersheds (Williams and Melack, 1991b). Comparisons of 10 pairs of snow samples with snowmelt waters flowing a short distance below the respective snowbanks led Feth et al. (1964b) to conclude that when snowmelt water comes in contact with the soil and rock, the initial diverse character of the precipitation largely disappears and the water rapidly increases in TDS content.

Eolian gypsum and halite are the probable source of $SO_4$ and Cl for some of the Group 1, 2 and 3 waters. Oxidation of pyrite is also a potential source of sulfur in the water samples. However, without more detailed study the relative contribution of pyrite oxidation cannot be quantified. This is also the case for leaching of intergranular salts or fluid inclusions of granitic rock minerals that potentially contribute Cl into the groundwater system. Fuge (1979) showed that unaltered granitic rocks from England and Scotland contain salts in which one- to two-thirds of the total Cl is soluble. Lacking better quantification of the mineral contribution of sulfur and chloride to the water chemistry, we will assume that all sulfur and chloride are from eolian sources, as do most prior workers (Garrels and MacKenzie, 1967; Thomas et al., 1989).

The evolution of precipitation (Table 6, no. 6) to Group-1 waters (Table 3) in the high Sierra Nevada can be explained by the weathering of a relatively small number of primary minerals found in the crystalline bedrock. An inverse model describing the evolution of precipitation (snow) to Group-1 water

can be written as:

Precipitation + Plagioclase + K-feldspar
+ Biotite or Forsterite + Halite + Gypsum
+ $CO_2$ gas → Ca–Na–$HCO_3$ water
+ Amorphous Silica + Kaolinite (Model 1)

Model 1 shows that the amounts of biotite and K-feldspar weathering are less than that of plagioclase (Table 5). This difference in weathering rates is in agreement with weathering rates of the respective silicate minerals given by Lasaga et al. (1994) and fits into a sequence of surface weathering proposed by Goldich (1938). Feth et al. (1964a), Garrels and MacKenzie (1967) have suggested that the weathering of feldspars and biotite and the formation of kaolinite largely account for the water composition in recharge areas. In the Sierra Nevada, weathering is enhanced by partial alteration and expansion of biotite, which results in disintegration of the crystalline rock (Wahrhaftig, 1965).

*5.3.3.2. Evolution of Group-1 Waters to Group-2 Waters*. Group-2 waters, which recharge the basin-fill aquifer, are found in lower slopes of the Sierra Nevada (generally below 2000 m) and dominate most of the Coso Range. Calcite and kaolinite become supersaturated in Group-2 water (Table 4). Given the climate and vegetation, water-rock interaction is assumed to be the principle mechanism for the evolution of water chemistry evolution of Ca–Na–$HCO_3$ (Group-1) water to Na–Ca–$HCO_3$ (Group-2) water.

An inverse modeling solution summarizing the evolution of Group-1 water to Group-2 water in the Sierra Nevada is:

Ca–Na–$HCO_3$ water + Plagioclase
+ K-feldspar or Biotite + Hornblende
or Forsterite + Halite + Gypsum
+ $CO_2$ gas → Na–Ca–$HCO_3$ water
+ Amorphous Silica + Calcite
+ Kaolinite (Model 2)

Based on the models (Table 5), dissolved constituents in the Group-2 waters come primarily from weathering reactions of plagioclase, biotite, and hornblende that form the granodioritic rocks and from dissolution of windblown halite and gypsum. Elevated magnesium concentrations in Group-2 waters are likely related to the weathering of magnesium-rich minerals (e.g. hornblende and biotite) that are commonly found in granodioritic rocks of the area (Miller and Webb, 1940; Hopper, 1947; Feth et al., 1964a; Wahrhaftig, 1965; Blum et al., 1994). However, increase in magnesium concentration in Group-2 waters (in the Coso Range area) is most likely due to abundance of olivine (forsterite) present (Duffield et al., 1980) in the basalt flow indigenous to the southern edge of the Coso Range.

*5.3.3.3. Evolution of Group-2 Waters to Group-3 Waters*. As Group-2 waters recharge the basin-fill aquifers and move toward central parts of the basins, concentrations of major-ions increase, producing Group-3 type water. Group-3 water is transitional in character, chemically as well as geographically, between Group-2 and Group-4 waters (Figs. 4 and 5). The increase in major-ion concentrations of Group-3 waters is a result of groundwater interactions with the basin-fill deposits. An inverse model for the processes is:

Na–Ca–$HCO_3$ water + Biotite
+ Forsterite + Halite + Gypsum + Na
from ion exchange + $CO_2$ gas
→ Na–$HCO_3$–Cl water + Ca or
Mg–Saponite + Calcite + Mg loss to
ion exchange. (Model 3)

The increase in playa deposits in areas where Group-3 waters dominate suggest that salt dissolution may be involved in the increases in Cl, Na, and $SO_4$ concentration. Weathering of the primary minerals results in the formation of smectite and calcite. Formation of smectite rather than kaolinite can be explained by the abundant supply of Mg from dissolution of volcanic materials such as forsterite, pyroxenes and basaltic

glass (Verhoogen et al., 1970). Since IWV is a geothermal area, $CO_2$ is assumed to be available along the flowpath.

*5.3.3.4. Evolution of Group-3 Waters to Group-4 Waters*. Groundwater in the alluvial basin-fill aquifer evolves from Na–$HCO_3$–Cl water to brackish Na–Cl water in the areas peripheral to playas (Figs. 4 and 5, Tables 3 and 5). These samples have a different geochemistry than Group-1 to -3 waters exemplified by increased TDS. The spatial correlation of the basin-fill and playa deposits with Group-4 samples suggests that lithology is important in the hydrochemical evolution. The increase in TDS is due to the relatively large increases in Na, Cl, and $SO_4$ concentrations suggesting that salt dissolution is the major control. An inverse model explaining the water chemistry along the flowpath can be written as:

Na–$HCO_3$–Cl water + Biotite

+ Forsterite + Halite + Gypsum + $CO_2$

gas + Na from ion exchange →

Na–Cl water + Mg–Saponite + Calcite

+ Mg loss to ion exchange (Model 4)

Most of the salt dissolution occurs as groundwater flows through the basin-fill deposits near playas. These sediments contain evaporative salts buried by sedimentation, which are mostly found in and around the playa lakes. Ion exchange is also common in basin sediments, with Ca and Mg ion concentrations increasing only slightly, whereas Na and K increase substantially along flowpaths (Table 3). Reader is referred to Güler (2002) for a more complete discussion of the modeling results.

The Coso Range is a geothermally active area (Duffield et al., 1980; Moore et al., 1982). This means that Group-3 water may be affected by mixing with water from geothermal leakage in the southern part of IWV (Whelan et al., 1989). This mixing scenario was explored by modeling mixtures between two geothermal waters from the Coso area and Group-3 water to create two synthetic Group-4 waters, called Mix 1 and Mix 2 (Fig. 8). Similarities between concentrations of some of the major and minor elements composing Mix 1 and Mix 2 and Group-4 water suggest that mixing may be part of the hydrochemical evolution. However, the present data are insufficient and more geothermal water analyses with more reliable minor element data are needed before a conclusive result can be determined.

*5.3.3.5. Evolution of Group-4 Waters to Group-5 Waters*. High TDS waters from across the area (represented by Group-4 and Group-5 water) are in parts of the aquifer that are in close proximity to the playa-areas. On the playa, high evaporation rates produce concentrated brine solutions, which lead to large horizontal and vertical density gradients in underlying groundwater. Tyler and Wooding (1991)

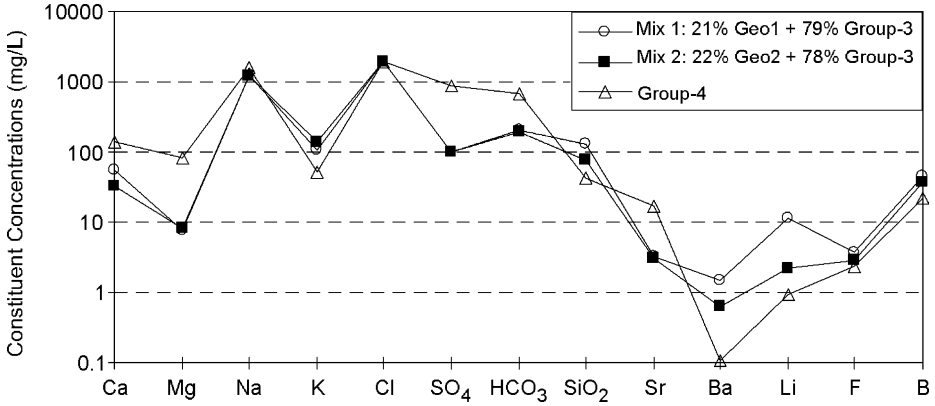


Fig. 8. Fingerprint diagram with aqueous parameters on x-axis versus concentration in mg/L on y-axis. Diagram shows result of mixing between two geothermal waters (Geo1 and Geo2) from the Coso geothermal wells with Group-3 water to try and create Group-4 water. Coso samples, Geo1 from CGEH Well No. 1, Geo2 from Coso Well No. 1, samples 9 and 13, respectively (Fournier et al., 1980).

suggested a mixing mechanism in playa areas via convective plumes or fingers, which develop into large-scale convection cells. Their field data suggested that convective fingering could be the dominant transport process for solutes in the groundwater beneath playas. A similar mixing mechanism was also suggested by Duffy and Al-Hassan (1988) for Pilot Valley in western Utah.

Attempts to match the Group-5 chemistry by evaporation of Group-4 water (PHREEQC simulation) failed, indicating that simple evaporation is not the only process occurring on the playas. In addition to evapotranspiration concentrating salts dissolved in the water the dissolution of salts found in the low permeability basin-fill deposits around playas is also an important process. The relatively high Na:Cl molar ratios of Group-4 and Group-5 waters (Na:Cl = 1.28 for both groups) suggest that the sodium and chloride contents of these samples is mostly derived from halite dissolution, which would result in a Na:Cl molar ratio close to one (Eugster and Jones, 1979; Yechieli et al., 1996). Group-4 samples are mostly from shallow wells (WS); (see Table 2) and these groundwaters move toward the playa as shallow subsurface flow (average depth of shallow wells is 28.4 m). In addition to evapotranspiration concentrating solutes at or very near the land surface, groundwater moving toward the surface also flows through salt deposits, which will dissolve increasing ion concentrations.

An inverse model explaining the water-chemistry can be written as:

Na–Cl water + Biotite + Halite + Gypsum + Nahcolite + Na from ion exchange → Na–Cl water + Kaolinite + Ca or Mg–Saponite + Ca and Mg loss to ion exchange. (Model 5)

The model includes dissolution of biotite, nahcolite and halite, precipitation of kaolinite and Ca or Mg–saponite and ion exchange (Ca and Mg replacing Na in clays) (Table 5). In summary, the inverse geochemical modeling demonstrated that relatively few phases are required to derive observed changes in water chemistry and to account for the hydrochemical evolution of groundwater in the area (Table 5). In a broad sense, the reactions responsible for the hydrochemical evolution of the groundwater fall into four categories: (1) silicate weathering reactions (e.g. feldspar and ferromagnesian mineral dissolution); (2) dissolution of salts (e.g. halite and nahcolite); (3) precipitation of calcite, amorphous silica and clays; and (4) ion exchange. The mineral phases were selected based on geologic descriptions and analysis of rocks (Table 1), descriptions of sediments from the area, stability diagrams (Fig. 7) and saturation data (Table 4). From the inverse modeling, knowing the exact weathering reactions is less important than knowing the overall stoichiometry (Wolford et al., 1996), which has been previously estimated for a part of the study area by Feth et al. (1964a); Garrels and MacKenzie (1967). These studies produced stoichiometries similar to those derived by this study (Table 5), but this study is the first to define inverse models for the complete flowpath, starting from recharge as precipitation in high Sierras to discharge on the playas.

### 5.4. Correlation of lithology and hydrochemical evolutions

Groundwater in the region generally begins as a $Ca–Na–HCO_3$ type in the recharge areas of Sierra Nevada, and chemically evolves along the flowpaths as a function of the lithologies encountered. Based on the saturation data, stability diagrams and inverse models, the composition of groundwater along a flowpath is primarily dependent upon (1) chemistry of the starting water; and the (2) types and relative solubility of the minerals available. We have not attempted to quantify the kinetic effects since mineral reaction rates and residence time of the water (short in mountain watersheds and long in alluvial basin-fill and playa deposits) is not well constrained.

Based on our work, the general lithology, including types and solubility of the minerals, constitutes the greatest controlling factor on the natural quality of the groundwater. To demonstrate this point, lithology frequencies for each water group were plotted by using the information

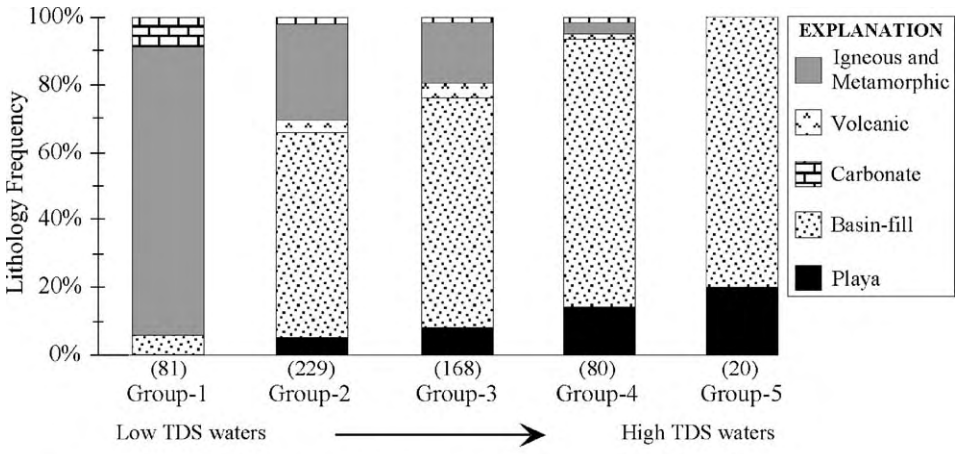


Note: Number in parenthesis shows the number of water samples in that particular group.

Fig. 9. Plots of water group versus lithology frequency (water groups determined from HCA results).

extracted from the GIS (Geographic Information Systems) database developed for this study. As shown in Fig. 9, TDSs content of the water groups rapidly increase as the percentages of basin-fill and playa deposits increase. This increase in concentration is probably due to the more soluble material in the basin-fill and playa deposits, coupled with the lower permeability of these sediments that increases the residence time of the groundwater.

## 6. Summary and concluding remarks

The results of this study show that analysis of hydrochemical data using statistical techniques such as cluster analysis coupled with inverse geochemical modeling of the statistical clusters can help elucidate the hydrologic and geologic factors controlling water chemistry on a regional scale. It should be noted that the cluster interpretations in this study are general and made on a regional basis. Because of this, there may be better interpretations within the context of a more localized system.

The spatial variations observed in the statistical groups correspond well to the topographic flowpaths. The physical locations and chemical evolution of groundwater represented by clusters Group-1, Group-2, Group-3, Group-4, and Group-5, follow the topographic flowpath: the recharge from the Sierra Nevada (Group-1 and Group-2) flows into the alluvial valleys, evolving through water-rock interaction into Group-3 water. Subsequently, Group-3 water flows to the discharge areas in and around the playa lakes, which usually occupy the central portions of the valleys, and evolve into discharge area waters (Group-4 and Group-5).

Systematic changes in water chemistry along the topographic flowpath were interpreted using saturation indices and mineral stability diagrams in order to formulate initial inverse models. Inverse modeling identified three distinct hydrochemical phases that can be attributed to water-rock interactions: (1) reactions of snowmelt water with minerals and $CO_2$ gas in recharge areas; (2) reactions of groundwater with aquifer material as it moves from recharge areas to discharge (playa) areas; and (3) reactions of discharging groundwater with playa minerals (see Table 5 for a complete list of minerals). It should be emphasized that the inverse modeling results are not unique, as for any hydrochemical evolution step more than one model is usually found. Effects of vegetation and microbial activity on the water chemistries have not been evaluated in this study, however, in areas like the Sierra Nevada, which has poorly developed soils and sparse vegetation, these effects are likely to be minimal.

We conclude that in the study area, chemical composition of the surface and ground water are

mainly controlled by: (1) climate and chemical composition of the precipitation; (2) aquifer lithology/mineralogy; (3) topography/physiography; and (4) physical aspects of the hydrogeologic system. These factors combine to create diverse water types that change in compositional character spatially and temporally as precipitation infiltrates the soil zone, moves down a topographically-defined flowpath and interacts with the minerals derived primarily from the underlying bedrock. Evaporative concentration and groundwater mixing appear to have lesser influence on the chemistry of the groundwater from the playa areas than salt dissolution. Finally, we assume that since reasonable inverse geochemical models were found for the topographic flowpaths, the statistically-defined hydrochemical facies can be used effectively to study the groundwater flow system and can be used as a tool to verify aquifer connectivity.

## Acknowledgements

The authors are thankful to the Editor and the reviewers for their valuable suggestions. This paper is based on part of the first author's dissertation research at the Colorado School of Mines, and he thanks members of his dissertation committee.

## References

Alberto, W.D., Del Pilar, D.M., Valeria, A.M., Fabiana, P.S., Cecilia, H.A., De Los Angeles, B.M., 2001. Pattern recognition techniques for the evaluation of spatial and temporal variations in water quality. A case study: Suquìa River Basin (Córdoba-Argentina). Water Res. 35, 2881–2894.

Alther, G.A., 1979. A simplified statistical sequence applied to routine water quality analysis: a case history. Ground Water 17, 556–561.

Back, W., 1966. Hydrochemical facies and ground-water flow patterns in northern part of Atlantic coastal plain. US Geol. Surv. Prof. Paper, 498-A.

Berenbrock, C., Martin, P., 1991. The ground-water flow system in Indian Wells Valley, Kern, Inyo, and San Bernardino Counties, California. US Geol. Surv. Water-Res. Invest. Rep., 89–4191.

Berenbrock, C., Schroeder, R.A., 1994. Ground-water flow and quality, and geochemical processes, in Indian Wells Valley, Kern, Inyo and San Bernardino Counties, California, 1987–88. US Geol. Surv. Water-Res. Invest. Rep., 93–4003.

Bethke, C.M., 1994. The Geochemist's Workbench, ver. 2.0: a User's Guide to Rxn, Act2, Tact, React, and Gtplot, University of Illinois, Urbana.

Bischoff, J.L., Menking, K.M., Fitts, J.P., Fitzpatrick, J.A., 1997. Climatic Oscillations 10,000–155,000 yr B.P. at Owens Lake, California reflected in glacial rock flour abundance and lake salinity in core OL-92. Quaternary Res. 48, 313–325.

Blum, J.D., Erel, Y., Brown, K., 1994. $^{87}Sr/^{86}Sr$ ratios of Sierra Nevada stream waters: Implications for relative mineral weathering rates. Geochim. Cosmochim. Acta 58, 5019–5025.

Christensen, M.N., 1966. Late Cenozoic crustal movements in the Sierra Nevada of California. Geol. Soc. Am. Bull. 77, 163–182.

Corbett, L., 1990. The weather at NWC-Climatological data for 1945–1989: Temperature, relative humidity, precipitation and evaporation, surface wind, station pressure, and solar radiation, China Lake, California. Naval Weapons Center Tech. Mem., 6738.

Drever, J.I., 1988. The Geochemistry of Natural Waters, Prentice-Hall, Upper Saddle River, NJ.

Droste, J.B., 1961. Clay minerals in sediments of Owens, China, Searles, Panamint, Bristol, Cadiz, and Danby Lake basins, California. Geol. Soc. Am. Bull. 72, 1713–1722.

Duffield, W.A., Smith, G.I., 1978. Pleistocene history of volcanism and the Owens River near Little Lake, California. J. Res. 6, 395–408.

Duffield, W.A., Bacon, C.R., Dalrymple, G.B., 1980. Late Cenozoic volcanism, geochronology, and structure of the Coso Range, Inyo County, California. J. Geophy. Res. 85, 2381–2404.

Duffy, C.J., Al-Hassan, S., 1988. Groundwater circulation in a closed desert basin: topographic scaling and climatic forcing. Water Resour. Res. 24, 1675–1688.

Dutcher, L.C., Moyle, W.R. Jr., 1973. Geologic and hydrologic features of Indian Wells Valley, California. US Geol. Surv. Water-Supply Paper, 2007.

ESRI (Environmental Systems Research Institute), 1996. Arc/View GIS Manual,.

Eugster, H.P., Jones, B.F., 1979. Behavior of major solutes during closed-basin brine evolution. Am. J. Sci. 279, 609–631.

Farnham, I.M., Stetzenbach, K.J., Singh, A.K., Johannesson, K.H., 2000. Deciphering groundwater flow systems in Oasis Valley, Nevada, Using trace element chemistry, multivariate statistics, and Geographical Information System. Math. Geol. 32, 943–968.

Fenneman, N.M., 1931. Physiography of Western United States, McGraw-Hill Book Company, New York.

Feth, J.H., Roberson, C.E., Polzer, W.L., 1964a. Sources of mineral constituents in water from granitic rocks, Sierra Nevada, California and Nevada. US Geol. Surv. Water-Supply Paper, 1535-I.

Feth, J.H., Rogers, S.M., Roberson, C.E., 1964b. Chemical composition of snow in the northern Sierra Nevada and other areas. US Geol. Surv. Water-Supply Paper, 1535-J.

Fournier, R.O., Thompson, J.M., Austin, C.F., 1980. Interpretation of chemical analyses of waters collected from two geothermal wells at Coso, California. J. Geophys. Res. 85, 2405–2410.

Frape, S.K., Fritz, P., McNutt, R.H., 1984. Water–rock interaction and chemistry of groundwaters from the Canadian Shield. Geochim. Cosmochim. Acta 48, 1617–1627.

Fuge, R., 1979. Water-soluble chlorine in granitic rocks. Chem. Geol. 25, 169–174.

Garrels, R.M., MacKenzie, F.T., 1967. Origin of the chemical compositions of some springs and lakes, In: Equilibrium Concepts in Natural Waters, American Cancer Society, Washington, DC.

Goldich, S.S., 1938. A study in rock-weathering. J. Geol. 46, 17–58.

Güler, C., 2002. Hydrogeochemical evaluation of the groundwater resources of Indian Wells-Owens Valley area, southeastern California [PhD. thesis]: Golden, Colorado School of Mines.

Güler, C., Thyne, G., McCray, J.E., Turner, A.K., 2002. Evaluation of graphical and multivariate statistical methods for classification of water chemistry data. Hydrogeol. J. 10, 455–474.

Hem, J.D., 1989. Study and interpretation of the chemical characteristics of natural water. US Geol. Surv. Water-Supply Paper, 2254.

Hollett, K.J., Danskin, W.R., McCaffrey, W.F., Walti, C.L., 1991. Geology and water resources of Owens Valley, California. US Geol. Surv. Water-Supply Paper, 2370-B.

Hopper, R.H., 1947. Geologic section from the Sierra Nevada to Death Valley, California. Geol. Soc. Am. Bull. 58, 393–432.

Howard, P.A., McAlee, J., Gillespie, J.M., 1997a. The role of fractures in surface and ground water flow: a field study of two canyons in the southeastern Sierra Nevada. Geol. Soc. Am. 29, 20(Abstracts with Programs).

Howard, P.A., Oehlschlager, E.K., Gillick, J., McAlee, J., Sherman, A.T., Ostdick, J.R., Steward, D.C., Gillespie, J.M., Thyne, G.D., 1997b. The Kern Plateau: a potential extra-basinal source of groundwater recharge to the Indian Wells Valley. Am. Assoc. Petrol. Geol. Bull. 81, 688(Pacific Section Meeting, Abstracts).

von Huene, R.E., 1960. Structural geology and gravimetry of Indian Wells Valley, southeastern California. PhD dissertation, University of California, Los Angeles.

Johnson, R.A., Wichern, D.W., 1992. Applied Multivariate Statistical Analysis, Prentice-Hall International, Englewood Cliffs, NJ.

Kistler, R.W., Bateman, P.C., Brannock, W.W., 1965. Isotopic ages of minerals from granitic rocks of the Central Sierra Nevada and Inyo Mountains, California. Geol. Soc. Am. Bull. 76, 155–164.

Kunkel, F., Chase, G.H., 1969. Geology and ground water in Indian Wells Valley, California. US Geol. Surv. Open-File Rept. without a number.

Lanphere, M.A., Dalrymple, G.B., Smith, R.L., 1975. K–Ar ages of Pleistocene rhyolitic volcanism in the Coso Range, California. Geology 3, 339–341.

Lasaga, A.C., Soler, J.M., Ganor, J., Burch, T.E., Nagy, K.L., 1994. Chemical weathering rate laws and global geochemical cycles. Geochim. Cosmochim. Acta 58, 2361–2386.

Lee, C.H., 1912. Ground water resources of Indian Wells Valley, California, California State Conservation Commission Rept., 403–429.

Lee, D.E., 1984. Analytical data for a suite of granitoid rocks from the Basin and Range province. US Geol. Surv. Bull., 1602.

Maxey, G.B., 1968. Hydrogeology of desert basins. Ground Water 6, 10–22.

McKee, E.H., Nash, D.B., 1967. Potassium–argon ages of granitic rocks in the Inyo batholith, east-central California. Geol. Soc. Am. Bull. 78, 669–680.

Meng, S.X., Maynard, J.B., 2001. Use of statistical analysis to formulate conceptual models of geochemical behavior: water chemical data from the Botucatu aquifer in São Paulo state, Brazil. J. Hydrol. 250, 78–97.

Miller, W.J., Webb, R.W., 1940. Descriptive geology of the Kernville quadrangle, California. Calif. J. Mines and Geol. 36, 343–378.

Moore, J.L., Austin, C.F., Prostka, H.J., 1982. Geology and geothermal energy development at the Coso KGRA, In: Transactions of third Circum-Pacific Energy and Mineral Conference, Honolulu: Circum-Pacific Council for Energy and Mineral Resources,.

Oliver, H.W., 1977. Gravity and magnetic investigations of the Sierra Nevada batholith, California. Geol. Soc. Am. Bull. 88, 445–461.

Parkhurst, D.L., Appelo, C.A.J., 1999. User's guide to PHREEQC (ver. 2)—A computer program for speciation, batch-reaction, one-dimensional transport, and inverse geochemical calculations. US Geol. Surv. Water-Resources Invest. Rept., 99–4259.

Parkhurst, D.L., Thorstenson, D.C., Plummer, L.N., 1980. PHREEQE-A computer program for geochemical calculations. US Geol. Surv. Water-Resources Invest. Rept., 80–96.

Piper, A.M., 1944. A graphic procedure in the geochemical interpretation of water-analyses. Trans., Am. Geophys. Union 25, 914–923.

Plummer, L.N., 1992. Geochemical modeling of water-rock interaction: past, present, future. In: Kharaka, Y.K., (Ed.), Proceedings of the Seventh International Symposium on Water-Rock Interaction, Amsterdam, pp. 23–33.

Plummer, L.N., Parkhurst, D.L., Thorstenson, D.C., 1983. Development of reaction models for ground-water systems. Geochim. Cosmochim. Acta 47, 665–686.

Plummer, L.N., Prestemon, E.C., Parkhurst, D.L., 1994. An interactive code (NETPATH) for modeling net geochemical reactions along a flow path. US Geol. Surv. Water-Resources Invest. Rept., 94–4169.

Saint-Amand, P., 1986. Water supply of Indian Wells Valley, California. Naval Weapons Center Tech. Pub., 6404.

SAS Institute, Inc, 1988. SAS/STAT user's guide, release 6.03 edn, SAS Institute Inc, Cary, NC, 1028.

Smith, G.I., 1962. Large lateral displacement on Garlock Fault, California, as measured from offset dike swarm. Bull. Am. Assoc. Petroleum Geologists 46, 85–104.

Smith, G.I., Friedman, I., McLaughlin, R.J., 1971. Studies of Quaternary saline lakes-III. Mineral, chemical, and isotopic evidence of salt solution and crystallization processes in Owens Lake, California, 1969–1971. Geochim. Cosmochim. Acta 51, 811–827.

StatSoft, Inc., 1995. STATISTICA for Windows [Computer program manual]. Tulsa, OK.

Stohlgren, T.J., Parsons, D.J., 1987. Variation of wet deposition chemistry in Sequoia National Park, California. Atmos. Environ. 21, 1369–1374.

Thomas, J.M., Welch, A.H., Preissler, A.M., 1989. Geochemical evolution of ground water in Smith Creek Valley—a hydrologically closed basin in central Nevada. USA Applied Geochem. 4, 493–510.

Tyler, S.W., Wooding, R.A., 1991. Experimental verification of convection of ground water beneath salt lakes. EOS Trans. 72, 216(Abstracts with Programs).

Verhoogen, J., Turner, F.J., Weiss, L.E., Wahrhaftig, C., Fyfe, W.S., 1970. The Earth, An Introduction to Physical Geology. Holt, Rinehart and Winsto, Inc.

Wahrhaftig, C., 1965. Stepped topography of the southern Sierra Nevada, California. Geol. Soc. Am. Bull. 76, 1165–1190.

Whelan, J.A., Baskin, R., Katzenstein, A.M., 1989. A water geochemistry study of Indian Wells Valley, Inyo and Kern Counties, California. Naval Weapons Center Tech. Pub., 7019.

White, A.F., Claassen, H.C., Benson, L.V., 1980. The effect of dissolution of volcanic glass on the water chemistry in a tuffaceous aquifer, Rainer Mesa, Nevada. US Geol. Surv. Water-Supply Paper 1535-Q.

Williams, R.E., 1982. Statistical identification of hydraulic connections between the surface of a mountain and internal mineralized sources. Ground Water 20, 466–478.

Williams, M.W., Melack, J.M., 1991a. Precipitation chemistry in and ionic loading to an Alpine basin, Sierra Nevada. Water Resour. Res. 27, 1563–1574.

Williams, M.W., Melack, J.M., 1991b. Solute chemistry of snowmelt and runoff in an Alpine basin, Sierra Nevada. Water Resour. Res. 27, 1575–1588.

Wolford, R.A., Bales, R.C., Sorooshian, S., 1996. Development of a hydrochemical model for seasonally snow-covered alpine watersheds: Application to Emerald Lake watershed, Sierra Nevada, California. Water Resour. Res. 32, 1061–1074.

Yechieli, Y., Ronen, D., Kaufman, A., 1996. The source and age of groundwater brines in the Dead Sea area, as deduced from 36Cl and 14C. Geochim. Cosmochim. Acta 60, 1909–1916.

Zbur, R.T., 1963. A geophysical investigation of Indian Wells Valley, California. Naval Ordnance Test Station Tech. Pub., 2795.